Towards Accurate and Wideband *In Vivo* Measurement of Skin Dielectric Properties

Yuan Gao, *Student Member, IEEE*, Mohammad Tayeb Ghasr, *Senior Member, IEEE*, Michael Nacy, *Student Member, IEEE*, and Reza Zoughi, *Fellow, IEEE*

***Abstract*— In this paper, we first review the most common measurement methods, previously used, for assessing the complex permittivity of human skin, namely, open-ended coaxial and waveguide probe reflectometry methods. We then outline and emphasize their useful features and shortcomings that can adversely affect the measurements. Then, an approach utilizing an open-ended waveguide probe with an engineered ground plane and a thin dielectric layer in front of the aperture to prevent skin protrusion is proposed. This approach utilizes a full-wave electromagnetic model that accurately describes the interaction of a layered skin with this probe. Furthermore, comprehensive analyses were performed to investigate the important sources of modeling and measurement errors and their influences on the calculated skin complex permittivity. The results of these analyses have shown that the proposed method can achieve ∼85% and ∼95% calculation accuracy for skin relative (to free space) dielectric constant and relative dielectric loss factor, respectively. Finally, a series of *in vivo* measurement was performed in the Ka-band (26.5–40 GHz) on several different locations of three human subjects using this proposed method. In addition, it is demonstrated that the homogeneous skin model cannot be used for areas of the body where the stratum corneum (SC) layer is relatively thick (e.g., palm). Finally, the effect of a thick SC layer on the relative complex permittivity calculation was discussed, and a modified method to determine the relative complex permittivity of the layered skin was proposed and verified by simulations.**

***Index Terms*— Dielectric properties, *in vivo*, reflectometry, relative complex permittivity, skin.**

I. Introduction

SKIN is the largest organ in the human body, and in addition to protecting body from the environment, it also regulates body temperature and moisture balance [1]. Skin is also susceptible to injuries (e.g., burns) and diseases (e.g., cancers). Recent investigations into using noninvasive high-frequency (i.e., microwave- and millimeter-wave) methods have shown tremendous potential for diagnosing such injuries and diseases [2]–[5]. For such purposes, proper knowledge of the electromagnetic properties of skin, primarily its complex permittivity, is critically important, since the changes in this parameter are closely related to the changes in its biophysical properties, especially its water content. Consequently, the changes in skin complex permittivity can yield information about skin cancer diagnosis and skin burn assessment [2]–[5]. Relative (to free space) complex permittivity is denoted by $\varepsilon_r = \varepsilon_r' - j\varepsilon_r''$, where ε_r' is the relative dielectric constant and ε_r'' is the relative dielectric loss factor. For brevity, hereon the word "relative" is assumed and omitted in the text.

In addition, the Federal Communications Commission (FCC) has approved the following new licensed frequency bands: 28 GHz (27.5–28.35 GHz), 37 GHz (37–38.6 GHz), and 39 GHz (38.6–40 GHz) and an unlicensed band at 64–71 GHz for the fifth generation communication needs [6]. Due to the high moisture content of skin, electromagnetic waves at these frequencies primarily interact with the skin layer and do not penetrate much beyond. Therefore, accurate information about skin complex permittivity is crucially important for evaluating dosimetry and for setting exposure limit standards. Therefore, a robust and accurate measurement method (including the corresponding complex permittivity calculation algorithm) suitable for *in vivo* human skin complex permittivity assessment is highly desired.

For the purpose of modeling the interaction of the skin with an electromagnetic wave, several skin models may be considered, as shown in Fig. 1(a)–(e) [7]–[9]. Human skin consists of three layers from the outermost to the innermost layer, namely, *epidermis*, *dermis*, and *subcutaneous fat* tissue. However, the top layer of epidermis that is called stratum corneum (SC), as shown in Fig. 1(a), represents the driest layer [7]. The rest of epidermis is referred to as the *viable epidermis* that has a similar water content to dermis. The complex permittivity of the skin is mainly affected by its water content. Thus, each skin layer with a different water content has a different complex permittivity. Normally, the epidermis is ∼0.06–0.1 mm thick, the dermis is ∼1.2–2.8 mm thick, and the SC layer is ∼20 μm thick [7], [8]. However, depending on the body location, SC may be somewhat thicker [10], [11]. Fig. 1(a) shows the most general layered structures of the skin, representing the situation where every layer has a different complex permittivity. Fig. 1(b) shows the homogeneous skin model that is the most simplified and widely used model. Fig. 1(c) shows the addition of the top dry SC layer to

Manuscript received March 7, 2018; revised May 17, 2018; accepted May 30, 2018. Date of publication July 16, 2018; date of current version December 24, 2018. This work was supported by the IEEE Instrumentation and Measurement Society Graduate Fellowship 2016–2017. The Associate Editor coordinating the review process was Samir Trabelsi. *(Corresponding author: Yuan Gao.)*

The authors are with the Applied Microwave Nondestructive Testing Laboratory, Department of Electrical and Computer Engineering, Missouri University of Science and Technology, Rolla, MO 65409 USA (e-mail: ygxgb@mst.edu; mtg7w6@mst.edu; michael.nacy@mst.edu; zoughi@mst.edu).

Color versions of one or more of the figures in this paper are available online at http://ieeexplore.ieee.org.

Digital Object Identifier 10.1109/TIM.2018.2849519

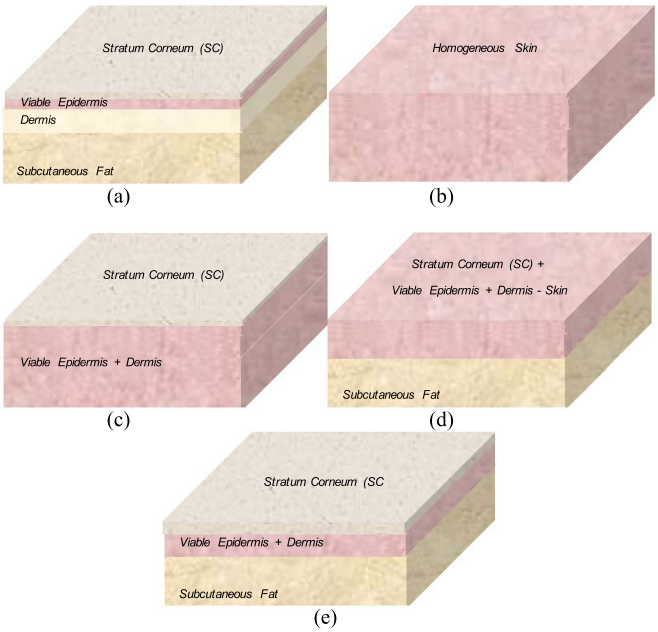

Fig. 1. Human skin model (not-to-scale) for different assumptions. (a) Four-layer model. (b) Homogeneous model. (c) Two-layer model assuming SC layer is not negligible but fat layer can be ignored. (d) Two-layer model for a situation that SC layer can be ignored but fat layer cannot. (e) Three-layer model for both SC and fat layer is taken into account (all not-to-scale). Viable epidermis is assumed, which has the same relative complex permittivity compared with dermis in the model (b)–(e).

the homogeneous model. Fig. 1(d) shows a two-layer model consisting of homogeneous skin and fat. Fig. 1(e) shows the addition of the top dry SC layer to the model in Fig. 1(d). In addition, *viable epidermis* and *dermis* are assumed to have the same complex permittivity in Fig. 1(b)–(e) and the bottom layers in all the models are infinitely thick. Finally, any electromagnetic model used must *correctly* and *accurately* represent the probe electromagnetic field characteristics and its subsequent interaction with a correct and representative model of the skin. To this end, in this paper, we first provide a thorough review of the previous works related to the skin complex permittivity measurement along with a discussion of each method's limitations and considered approximation which are seldom quantitatively discussed.

Subsequently, we fully describe and analyze the implementation of an open-ended rectangular waveguide probe to evaluate the complex permittivity of human skin *in vivo*. However, contrary to previously implemented methods using the same probe, the approach outlined here uses a *full-wave* electromagnetic model that fully describes the interaction of a wideband signal radiated by this probe into a layered model of human skin [12]. This method provides for the correct calculation of the complex permittivity (and thickness if need be) of a given layer within the skin structure. In addition, and as will be seen later, this model properly (i.e., no approximation) facilitates the use of a known additional layer of a material, placed in front of the open-ended waveguide aperture to prevent skin from protruding into the waveguide, which is an extremely critical issue. As a result, we first thoroughly discuss the relevant practical issues associated with using an open-ended waveguide probe for measuring skin complex permittivity *in vivo*. This includes concerns and remedies over the effects of: 1) approximating probe electromagnetic field modes and the influence of waveguide ground plane (flange) edge reflections resulting in errors in the measured reflection coefficient, which is then used to calculate the complex permittivity from these measurements and 2) pressure (on the skin) that is used in the measurements. Then, the possible sources of complex permittivity calculation errors are discussed, including using: 1) homogeneous assumption for skin; 2) errors in the thickness and complex permittivity of the additional layer placed between the waveguide probe and the skin to prevent skin protrusion into the waveguide; and 3) instrument noise and (operator) measurement inconsistency. Subsequently, *in vivo* human skin measurements are conducted on three human subjects and on several different locations within their bodies. Finally, the effect of a thick SC layer in the complex permittivity calculation is discussed, and then, a modified method suitable for a general layered structure is proposed and verified by simulation.

II. Background of Human Skin Complex Permittivity Measurement

Currently, the most commonly used skin complex permittivity measurement method involves measuring the reflection coefficient of skin in contact with an open-ended coaxial or a rectangular waveguide probe. Subsequently, the measured reflection coefficient is used in conjunction with an electromagnetic model that describes the measurement environment to extract the complex permittivity. A comprehensive review of complex permittivity measurement of biological tissues, including human skin, was conducted in 1996 [13], and the review below mainly focuses on the subsequent progress in this field.

The application of the open-ended coaxial probe is relatively easy and measuring dielectric properties of certain materials (i.e., infinite half-spaces and liquids) has been well documented [14], [15]. A series of investigations was conducted in the 1990s with respect to determining human skin complex permittivity using the open-ended coaxial probes [16]–[18]. *In vivo* measurements of a reflection coefficient were first performed with this probe on human palm, forearm, and sole of foot in the frequency range of 10 Hz–20 GHz. Subsequently, skin complex permittivity at these locations was calculated based on the admittance model of the coaxial probe [19]. Finally, a parameterized Cole–Cole model was developed by *curve fitting* the complex permittivity results below 20 GHz. Then, the complex permittivity values at higher frequencies were obtained by *extrapolating* the lower frequency results [18]. A similar method was used to measure and calculate the complex permittivity of palm and wrist epidermis in 0.5–110 GHz by a small coaxial probe [20]. However, in this paper, it is assumed that only epidermis layer is sampled by the electric field of the probe. In addition, the approach used to determine the sampled thickness is performed on pork fat and muscle, so the obtained quantitative results do not apply to human skin. It is also not clear whether the results are obtained *in vivo* or performed on the excised skin.

Chahat *et al.* [21] used a commercial measurement system to conduct *in vivo* complex permittivity measurements on human palm, wrist, and forearm in the 10–60 GHz frequency range. The major disadvantage of the admittance model-based open-ended coaxial probe method is that it assumes human skin to be homogeneous (only a single layer), which is not necessarily a correct assumption (particularly as a function of body location) and can lead to errors in calculating the complex permittivity. For example, a reflection coefficient measured on forearm/wrist and palm with an open-ended coaxial probe could be substantially different, since palm usually has a thicker and drier SC layer [17], [20], [21]. In addition, the penetration depth of a coaxial probe is proportional to its diameter. Thus, to eliminate the influence of the existing fat layer below the skin, a small-diameter coaxial probe is usually used to assure that the field sampling depth is in the skin layer only. However, using such a coaxial probe and when the SC layer is relatively thick, viable epidermis and dermis layers may not be sufficiently exposed to the probe fields. All these reasons result in a lower-than-expected calculated complex permittivity of skin [17], [21].

The issue of skin inhomogeneity is mentioned by several researchers, and attempts have been made to consider the layered nature of skin. However, using a static admittance model limits the application to only several hundred megahertz [22]–[25]. Sasaki *et al.* [26], [27] employed several different methods, including open-ended coaxial probe reflectometry, to determine the complex permittivity of different skin layers. However, the measurements were performed on the dissected porcine skin. This method is not suitable for establishing *in vivo* human skin complex permittivity due to the destructive nature of the measurements. To properly model the interaction between the open-ended coaxial probe and the layered skin structure, a wave propagation model is needed, such as the one developed in [28]. Furthermore, an appropriate calculation algorithm is needed to properly extract the complex permittivity and/or thickness of each layer. Unfortunately, up to date, no such effort has been reported. Finally, calibrating an open-ended coaxial probe for measuring the reflection coefficient of nonliquid materials is not a straightforward process, and any errors due to calibration can significantly and adversely affect the measurement results [29]. This limits the potential of using a coaxial probe for complex permittivity determination in a general layered structure.

Open-ended waveguide probes have also been used as an effective tool to obtain thickness and complex permittivity of the layered dielectric materials [12], [30], [31]. Alekseev *et al*. [8] utilized the open-ended waveguide probes to measure the *power* reflection coefficient (not the complex reflection coefficient) of human skin and subsequently obtained skin complex permittivity and thickness by *curve fitting* the measured data. In that work, different multilayer skin models were proposed, and the results were shown that the multilayer model gives better fitting results compared with the homogeneous model (i.e., assuming skin to be a single homogeneous layer). Although the results were shown good agreement with other cited references in the literature, a transverse electromagnetic (TEM) wave assumption was used in the calculation, which is not the case in reality. That is to say that this assumption: 1) does not properly account for the complex interaction of the EM field in the near field of a waveguide probe with a skin layer(s) and 2) it ignores the ever-important higher order modes that are generated at the aperture, all of which lead to inaccuracies when calculating the complex permittivity of skin [12]. The consequences of these critical issues on the calculated skin thickness and complex permittivity are also not discussed in detail. Hey-Shipton *et al*. [32] measured human palm *in vivo* at 8–18 GHz with a waveguide probe and polystyrene plug to prevent skin protrusion into the open-ended waveguide probe. However, when calculating skin complex permittivity, they ignored the presence of the plug (i.e., assuming plug has a complex permittivity equal to that of free space), which is not the case. In addition, they also used the infinitely thick skin layer (i.e., homogeneous) model for human palm. Ghodgaonkar *et al.* [33] and Tamyis *et al.* [34] measured human palm *in vivo* with a waveguide probe and a Teflon impedance transformer. However, again a homogeneous model is used for the palm skin. In addition, a transmission line assumption was used to account for the presence of the Teflon impedance transformer, which is not accurate when dealing with radiation through an open-ended waveguide probe. This constitutes only an approximation, which can significantly impact the calculation of complex permittivity. Moreover, the measurements were conducted with a waveguide probe with a finite flange, but an infinite flange formulation was used for calculation, and this may also lead to additional errors in complex permittivity calculation, as described in [35].

Another important practical issue to consider, when using an open-ended waveguide probe, is that when measuring soft materials, such as skin, the applied pressure can result in significant errors as a consequence of tissue protrusion into the waveguide aperture. Several solutions have been proposed to overcome this critical concern, such as using some variations of a plug [32]–[34], [36]. However, in all cases, the above-discussed issues remain unresolved. A filled waveguide solution was also proposed to solve the pressure problem, but only for measuring the reflection coefficient of healthy skin to be compared with an unhealthy skin (i.e., not for calculating skin complex permittivity) [37], [38].

Several other methods have also been used for determining skin complex permittivity. Time-domain spectrometry has been used to measure excised healthy and wounded skin complex permittivity in the frequency range of 10 MHz–10 GHz [39]. The free-space transmission method is used in the frequency range of 60–100 GHz for excised human skin [40]. However, these two studies are invasive and not applicable to *in vivo* measurements. The secondary effect of an electromagnetic wave interaction with skin, such as thermal effect, is also utilized to determine the power density and penetration depth in the skin, and then, the penetration depth is used for complex permittivity calculation [41]. However, this method is only verified for a single frequency.

The above-mentioned measurement approaches have their respective limitations and considered approximations that affect the outcome of calculating the complex permittivity

of skin to varying degrees. Unfortunately, the influence of these limitations and approximations on complex permittivity calculation results is seldom discussed. Consequently, a more robust and accurate measurement methodology with a comprehensive discussion of calculation accuracy analysis is desired, particularly for *in vivo* skin measurements.

III. Practical Problems and Their Remedies Using an Open-Ended Waveguide Probe for Skin Measurements

A. Influence of Field Distribution Assumption and Finite Ground Plane Edge Reflections on Skin Complex Permittivity Measurements

As mentioned in Section I, when using open-ended rectangular waveguide probes for skin complex permittivity measurements, the previously implemented irradiating wave model has been either free-space TEM mode or transmission line model for impedance matching in a portion of the overall measurement probe. In addition, when a waveguide admittance model used (non-TEM), the influence of higher order modes present at the waveguide aperture has been ignored. Neglecting these important facts can result in significant errors in calculating complex permittivity.

As part of a broader and more general investigation of radiation of electromagnetic waves into layered composite structures, a comprehensive forward model and inverse (forward-iterative) algorithm for a waveguide probe interaction with multilayer structures was developed in [12]. This model is capable of accurately producing the complex reflection coefficient, referenced at the waveguide aperture, for an open-ended rectangular waveguide probe radiating into a generally lossy layered structure. Specifically, the model accounts for the presence of higher order modes in addition to the dominant TE_{10} mode for proper electromagnetic field matching at the waveguide aperture. Higher order modes are generated at the waveguide aperture and contribute to the complex reflection coefficient from which the thickness and complex permittivity of each layer are subsequently calculated.

To show the differences in calculating the complex reflection coefficient, at the waveguide aperture, using only TEM waves, only waveguide TE_{10}, and addition of 14 higher order modes to the dominant TE_{10} mode, Fig. 2(a) shows the simulated complex reflection coefficient of skin at the *Ka*-band (26.5–40 GHz). These are also compared with the results obtained by a full-wave electromagnetic model using CST Microwave Studio. For the purpose of this comparison, the skin was assumed to be thick and homogeneous with its complex permittivity given in [18] (for nonwet skin). The results clearly indicate that the TEM wave assumption results in a significant error in a simulated reflection coefficient compared to when proper waveguide aperture irradiating wave model is used. The CST Microwave Studio simulated reflection coefficient was used to calculate the complex permittivity of the skin by using the TEM model, open-ended waveguide model with 1 and 15 modes, respectively. The calculated results are shown in Fig. 2(b) and (c). As the results shown in Fig. 2, the error in calculating both the dielectric constant

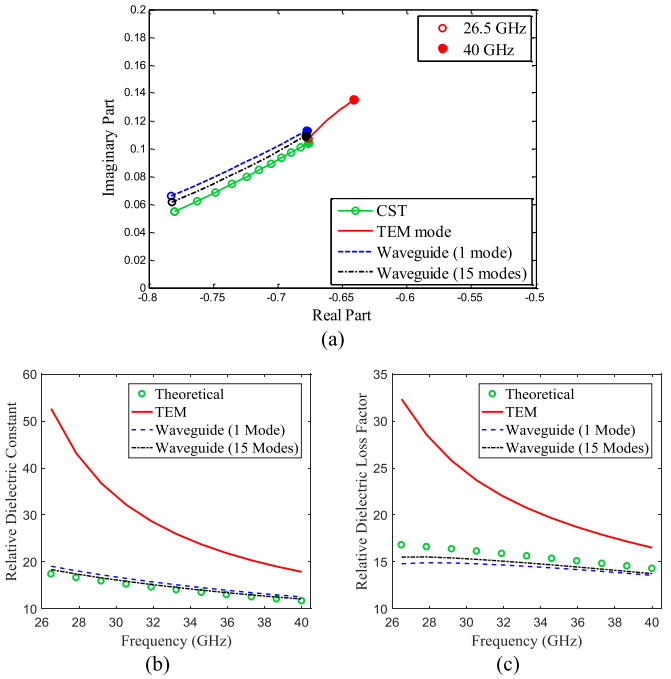

Fig. 2. (a) Simulated reflection coefficient of homogeneous skin for different irradiating wave modes including CST results, (b) calculated relative dielectric constant, and (c) calculated relative dielectric loss factor with different models.

and the dielectric loss factor can be very substantial. The results also indicate that this difference in complex permittivity calculation is a function of frequency and decreases as frequency increases. In addition, the results in Fig. 2 show that ignoring the presence of higher order modes affects the results less significantly than the TEM wave assumption because of the high loss nature of complex permittivity used for this comparison [12].

In this paper, a calculation error is defined by

$$\text{Calculation Error} = \left| \frac{\varepsilon_{\text{Theoretical}} - \varepsilon_{\text{Calculated}}}{\varepsilon_{\text{Theoretical}}} \right| \times 100\% \qquad (1)$$

where $\varepsilon_{\text{Theoretical}}$ is the theoretical dielectric constant or dielectric loss factor used in the simulation, and $\varepsilon_{\text{Calculated}}$ is the calculated dielectric constant or dielectric loss factor.

Another consideration, when using open-ended rectangular waveguide probes, has to do with the fact that all (forward) models assume an infinite ground plane at the waveguide aperture, while the measurements are instead conducted with finite-sized ground planes (i.e., waveguide flanges). Reflections caused by the edges of a finite-sized flange also contribute to errors in the measured reflection coefficient compared with those derived from the models. This in turn leads to additional sources of error when calculating complex permittivity. One effective solution to this problem is the use of a modified (engineered) flange that closely represents the electromagnetic characteristics of an infinite ground plane used in the modeling and simulations [35]. Fig. 3 shows a picture of an open-ended waveguide probe with a standard (finite-sized) flange (left) and a modified (engineered) flange (right), respectively.

Therefore, throughout this paper and in all reported simulation results, higher order modes (15 modes) are considered and all measurements are conducted with the engineered flange to

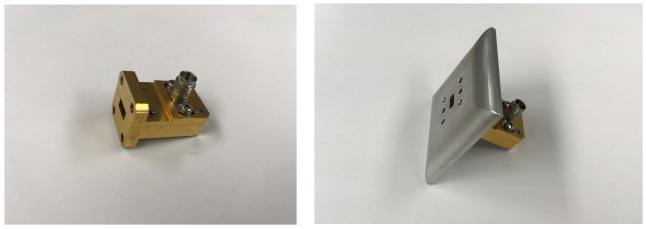

Fig. 3. Open-ended waveguide probe with a standard (finite) flange (left) and a modified (engineered) flange (right).

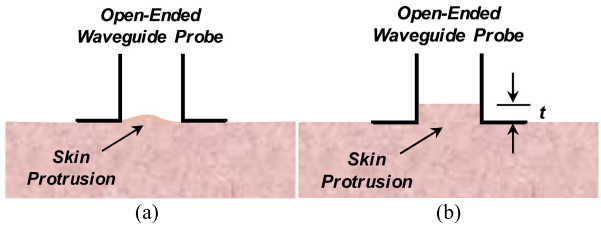

Fig. 4. (a) Illustration of skin protrusion problem. (b) Simulation model in which pressure on skin is represented by its protrusion inside the waveguide probe and its effective thickness, t.

significantly reduce any errors associated with their respective issues, as discussed earlier. Furthermore, the algorithm for calculating the reflection coefficient (forward model) and calculating complex permittivity used in this paper is the same as the one given in [12]; otherwise, more description will be given.

B. Influence of Applied Pressure on Skin Complex Permittivity Measurements

Skin is a soft tissue. Consequently, it is necessary to apply some pressure to assure that the open-ended waveguide aperture is completely covered by the skin tissue. However, this pressure causes the skin to protrude into the waveguide to some degree, as shown in Fig. 4(a). This will significantly affect the measured complex reflection coefficient, which in turn leads to significant errors in the calculated complex permittivity of the skin. To illustrate the importance of the need to account for and remedy this practical issue, a corresponding simulation model was constructed using CST Microwave Studio at the *Ka*-band (26.5–40 GHz), as shown in Fig. 4(b). For this illustration, skin is assumed to be homogeneous and its complex permittivity is again set equal to that given in [18]. In this model, variations in the complex reflection coefficient, caused by skin protrusion, were calculated as a function of the effective thickness of protruding skin tissue (i.e., t) inside the open-ended waveguide probe, as shown in Fig. 4(b).

The simulated results in Fig. 5 show that even a very slight amount of pressure, represented by a skin protrusion of $t = 0.2$ mm, can cause a significant change in the complex reflection coefficient of the skin, especially in its phase, as expected. However, what is more important is the effect of this pressure on the calculated complex permittivity of skin. To show this adverse influence, the results shown in Fig. 5 for $t = 0$ mm and 0.2 mm were used to calculate the complex permittivity of skin using the algorithm given in [12]. The calculated results are compared with the theoretical value

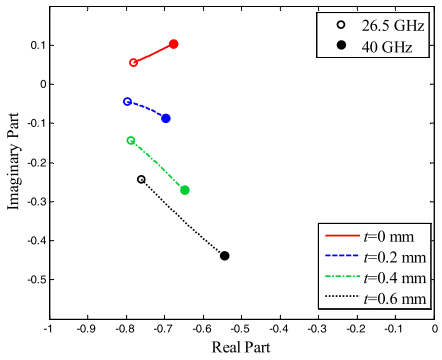

Fig. 5. Simulated reflection coefficient results for different amounts of pressure represented by t in Fig. 4(b).

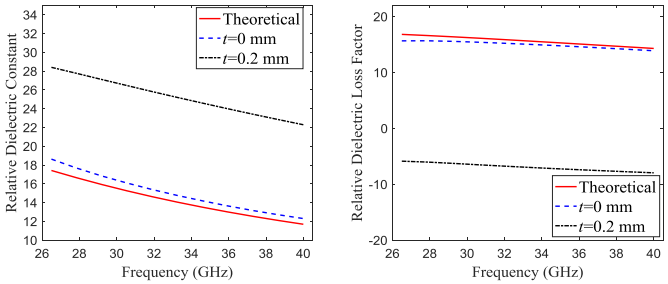

Fig. 6. Calculated relative complex permittivity based on the full-wave simulated reflection coefficient. (a) Relative dielectric constant. and (b) Relative dielectric loss factor.

(complex permittivity used in the full-wave simulation) in Fig. 6. Results show that when no skin tissue protrudes into the waveguide ($t = 0$ mm), the calculated complex permittivity is very close to the theoretical value, as expected. The slight differences are due to the numerical calculation error associated with the full-wave simulation. On the other hand, when even a slight amount of skin tissue protrudes into the waveguide ($t = 0.2$ mm), the calculated complex permittivity is very different than the theoretical values, even resulting in an erroneous negative dielectric loss factor values over the frequency range. The results clearly show that the reflection coefficient error caused by pressure can lead to significant complex permittivity calculation error.

A rigid additional dielectric material layer can be added in front of the open-ended waveguide aperture to prevent skin protrusion into the waveguide. Then, using the algorithm given in [12], which properly accounts for the presence of this layer, one can accurately calculate the skin complex permittivity if the thickness and the complex permittivity of this additional layer are known. This fact will be shown later along with a discussion of the sensitivity of skin complex permittivity calculation as a function of the thickness and complex permittivity of this layer.

IV. Consideration of Potential Sources of Complex Permittivity Calculation Error in the Proposed Method

A. Error Caused by Using Homogeneous Skin Assumption

Skin is commonly assumed to be homogeneous at microwave- and millimeter-wave frequency bands because of

the limited penetration depth into the skin at these frequencies. However, the quantitative analysis of complex permittivity calculation error caused by this assumption is seldom reported and remains unknown.

Using the homogeneous skin model means that the influences of dry SC layer and the subcutaneous fat layer are ignored. The conditions under which this assumption is valid are: 1) the SC layer is very thin, so its contribution to the total reflection coefficient is negligible and 2) the (lossy) skin layer is relatively thick, so that the incident wave either does not reach the fat layer or any reflections from that layer is substantially attenuated.

Here, we analyze the effects of the presence of SC and fat layers. The reflection coefficient of the skin model given in Fig. 1(e) is calculated as a function of SC layer thickness, and different thickness of the viable epidermis and dermis layers together, hereon referred to as the second layer. The subcutaneous fat layer is assumed to be infinitely thick. The complex permittivity of an SC layer is set to that of palm SC layer given in [8]. Complex permittivity of the second and the fat layers is set to those of skin and infiltrated fat given in [18], respectively. Subsequently, this reflection coefficient is used to calculate the complex permittivity by assuming that the skin is homogeneous. The maximum complex permittivity calculation error in the *Ka*-band frequency range of 26.5–40 GHz caused by the homogeneous skin assumption is then calculated. This is done by first calculating the error for each frequency point as determined by (1). Then, the maximum value in this range is denoted as the maximum complex permittivity calculation error. The results are presented in Fig. 7.

Several conclusions can be drawn from these results as follows.

1) The calculation error generally decreases as a function of increasing second layer thickness. This is due to the losses in the second layer, reducing the effect of the third (fat) layer on the overall reflection coefficient. However, this relationship is not a linear one as a function of the second skin layer thickness [12].
2) When the effect of a fat layer is significantly reduced, complex permittivity calculation error increases as a function of increasing the SC layer thickness, as expected.

Since human skin has ∼0.02-mm-thick SC layer and the second layer is usually larger than 1.2 mm, the maximum calculation error caused by the homogeneous skin assumption is less than ∼15% in the *Ka*-band (26.5–40 GHz) frequency range. This error decreases to less (∼5%) when the second layer is thicker than ∼1.6 mm. Thus, the results indicate that if these levels of error are acceptable for a given application, then using the homogeneous skin model in the *Ka*-band (26.5–40 GHz) frequency range when performing open-ended waveguide measurements should be fine. Furthermore, as will be shown later, if the thickness of each layer of skin is also available (through secondary measurement means), then more accurate results can be obtained.

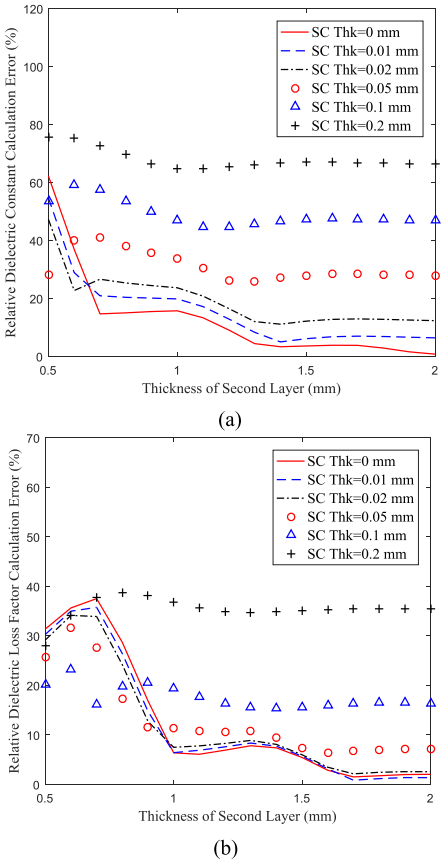

Fig. 7. Maximum (a) relative dielectric constant and (b) relative dielectric loss factor calculation error in the *Ka*-band frequency range, when a homogeneous skin model [Fig. 1(b)] is used in calculating skin relative complex permittivity in place of the layered model [Fig. 1(e)].

B. Sensitivity to the Thickness of Additional Layer

To closely calculate skin complex permittivity, the thickness and complex permittivity of the additional layer, used to prevent skin protrusion into the waveguide, must be accurately known. The optimum thickness and the complex permittivity of this layer change as a function of frequency and the properties of the layered structure to be examined [12]. Therefore, a careful analysis must be performed to evaluate the sensitivity of skin complex permittivity calculation to the additional layer thickness and complex permittivity. Thus, to evaluate the sensitivity of skin complex permittivity calculation to these parameters, a two-step approach was followed.

In the first step, a reflection coefficient was calculated in the *Ka*-band (26.5–40 GHz) frequency range for a two-layer model (i.e., the additional layer and homogeneous skin) while changing the thickness of the former about a nominal value with a given percent thickness error (i.e., maximum uncertainty in knowing the actual thickness) about the nominal value. The additional dielectric layer was assumed to be lossless and its relative dielectric constant was set as 2, mimicking those of most polymers and paper products from which this layer may consist. As before, the skin complex permittivity was set to that given in [18].

In the second step, the calculated reflection coefficient in step 1 was used to calculate skin complex permittivity by

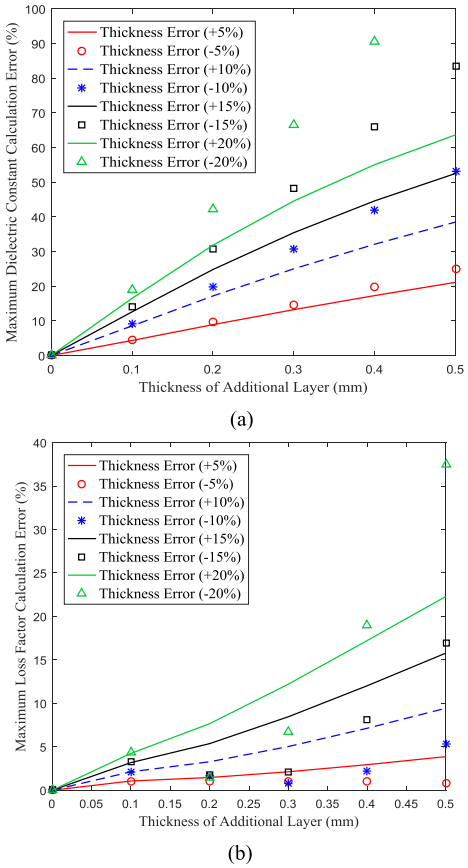

Fig. 8. (a) Relative dielectric constant calculation error and (b) relative dielectric loss factor calculation error caused by inaccuracy in knowing the additional layer thickness with the relative dielectric constant of the additional layer set at 2.

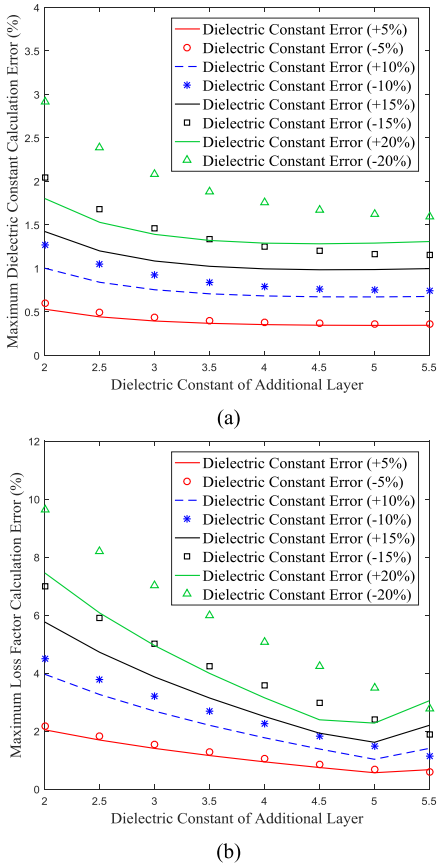

Fig. 9. (a) Relative dielectric constant calculation error and (b) relative dielectric loss factor calculation error caused by a relative dielectric constant error of the additional layer, where the additional layer thickness is 0.1 mm, and its relative permittivity varies from 2 to 5.

assuming that the top dielectric layer has a thickness equal to the exact nominal thickness and its relative dielectric constant. In this way, the sensitivity of skin complex permittivity calculation to any deviation from the assumed nominal thickness can be investigated (i.e., sensitivity to the thickness of this additional layer). The maximum complex permittivity error within the *Ka*-band (26.5–40 GHz) frequency range was again calculated by comparing the results with the skin complex permittivity used in the reflection coefficient calculation. The results, presented in Fig. 8, show that the skin complex permittivity calculation error is quite sensitive to the thickness error associated with the additional dielectric layer. Also, the complex permittivity error for a given percent thickness error generally increases as a function of increasing additional layer thickness. In other words, and based on the results in Fig. 8, the additional layer needs to be relatively thin and has a small thickness error associated with it (i.e., well produced). To this end, materials such as ordinary paper, which has a low relative dielectric constant (∼2), is loss less, and has a precise thickness (with respect to its actual thickness) could be a good candidate for this purpose.

C. Sensitivity to the Complex Permittivity of the Additional Layer

A similar approach was followed to analyze the calculation error of skin complex permittivity caused by the error (i.e., maximum uncertainty in knowing the actual complex permittivity) in the complex permittivity of the additional layer. First, the reflection coefficient was calculated in the *Ka*-band (26.5–40 GHz) for a two-layer model consisting of a 0.1-mm-thick additional dielectric layer and an infinitely thick skin layer, while the dielectric constant of the additional layer (assumed lossless) was varied. Similar to the thickness analysis, the dielectric constant of the additional layer was varied by a certain percentage about a nominal value. Then, the calculated reflection coefficient was used to calculate the complex permittivity of the skin layer by assuming that the additional layer dielectric constant equals that of its nominal value. The maximum calculation error within the *Ka*-band frequency range (26.5–40 GHz) was then calculated by comparing the calculated complex permittivity with the skin complex permittivity used in the reflection coefficient calculation. The results, presented in Fig. 9, show that unlike the sensitivity shown by the calculated complex permittivity to the additional layer thickness, the calculation results are much less sensitive to variations about the nominal dielectric constant values of the additional layer.

In conclusion, in order to minimize the calculation error due to the introduction of the additional layer, it must be thin, and its thickness and dielectric constant errors must also be small. The complex permittivity of such materials may

be readily and accurately measured using several well-known techniques [12], [42].

D. Sensitivity to Instrument Noise and Measurement Inconsistency

Another source of complex permittivity calculation error is instrument noise and measurement inconsistency associated with the operator. The effect of instrument noise can be significantly reduced by using a high-quality and "low noise" instrument, such as commercial vector network analyzer (VNA), coupled with a high-quality calibration standard and process. Measurement inconsistency can be determined and improved by performing multiple measurements (i.e., averaging of the measured data) and using multiple skilled operators.

When a custom-designed measurement system is used (i.e., not a high-quality commercial VNA), the noise level of the system needs to be measured, and the corresponding calculation error caused by this noise level must be investigated. In addition, several reflection coefficient measurements and subsequent complex permittivity calculation should be performed and the results should be averaged. This helps in reducing the influence of operator measurement inconsistencies and better ascertains the robustness of the measurement method and the calculation algorithm. Unfortunately, the influence of these factors has seldom been discussed previously (see [8]). Furthermore, although the average and standard deviation of the measured reflection coefficient may be given in the previous studies, and the corresponding complex permittivity calculation standard deviation is absent. Given the nonlinear relationship between the two, this effect can be significant and must be investigated. Gabriel *et al.* [16] mention that the complex permittivity calculation results could be within $\sim \pm 5\% - \pm 10$ % for their measurements at frequencies higher than 100 MHz. However, the reason given for this variation is the inhomogeneous nature of skin without any further or evidential analysis. However, the recent results of research using the similar approach for measuring skin tissue show that the standard deviation for dielectric constant and dielectric loss factor could be as high as 16.9% and 26.1%, respectively [5].

As will be shown later, in this paper, we performed several reflection coefficient measurements, at every location on the human subjects used, in addition to using multiple operators confirming each other's measurement results, as will be shown later. It was concluded that measurement inconsistency due to multiple measurements and using different operators was insignificant. This was partially due to the fact that they were skilled operators in using VNAs, the calibration process.

As it relates to reflection coefficient measurements using a VNA, the minimum measurable signal (noise floor) can be considered as the residual calibration errors that are determined by the quality of the calibration standards used (in particular the matched load). Since these residual signals have small amplitudes, they can be lumped with other sources of instrument noise as an additive white Gaussian noise (WGN), N, to the ideal measured reflection coefficient, which is given as

$$\Gamma = \Gamma_{\text{ideal}} + N$$

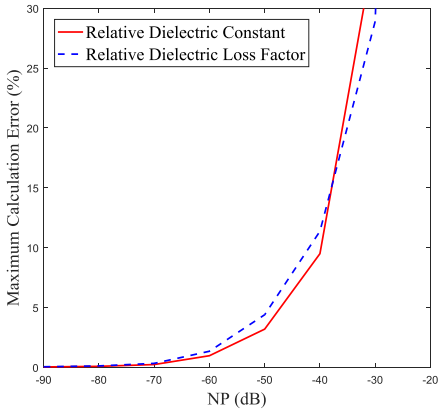

Fig. 10. Maximum relative complex permittivity calculation error in the homogeneous skin model caused by different noise levels.

where Γ is the measured complex reflection coefficient and Γ_{ideal} represents the complex reflection coefficient free of instrument noise. Thus, to quantitatively investigate the effect of instrument noise on complex permittivity calculation, noise power (NP) in the reflection coefficient averaged over the frequency band given was used

$$\text{NP} = 10\log_{10}\frac{\sum_{i=1}^{n}|N(i)|^2}{n}\ (\text{dB})$$

where i is the ith measurement frequency sampling point.

To determine the influence of instrument noise on a maximum complex permittivity calculation error, simulations were performed for the homogeneous skin model at the *Ka*-band (26.5–40 GHz). First, the reflection coefficient of the homogeneous skin model, Γ_{ideal}, was calculated. The skin complex permittivity is set as that given in [18], and then, WGN with different NP levels was added to Γ_{ideal} to obtain Γ. Then, Γ was used to calculate the complex permittivity. Subsequently, the complex permittivity calculation error was obtained by comparing the calculation results with the theoretical complex permittivity, resulting in the relationship between the maximum complex permittivity calculation error (within the frequency band) and the NP level, as shown in Fig. 10. The results show that the maximum complex permittivity calculation error rapidly increases for NP levels greater than -50 dB. This puts restrictions on the quality of the calibration standards used and the instrument itself. The system used in this paper is consisted of a calibrated Anritsu MS4644A VNA, modified *Ka*-band (26.5–40 GHz) open-ended rectangular waveguide probe, and a semirigid coaxial cable. The NP for this instrument was obtained by measuring the reflection coefficient of a matched load (where $\Gamma_{\text{ideal}} = 0$), as explained earlier. The measurements were conducted five times, and the NP was varied between -50.1 and -46.4 dB with an average of -47.8 dB. According to the results shown in Fig. 10, the calculation error caused by the instrument noise may be as high as $\sim$7%.

E. Estimation of Calculation Accuracy Due to Multiple Sources of Error

In practice, more than one source of error may exist in a given measurement. Therefore, it is important to assess or

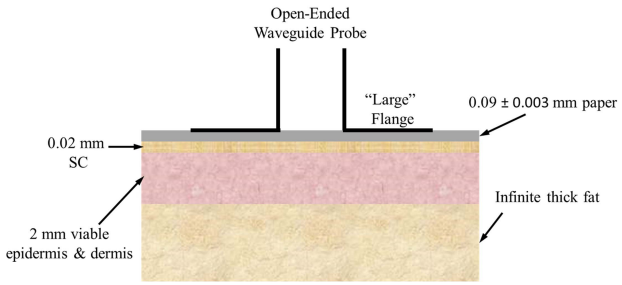

Fig. 11. Simulation model used for estimating calculation errors due to multiple sources of error.

estimate the complex permittivity calculation accuracy with multiple sources of error present. We can estimate the calculation accuracy using the previous derivation. Here, the total error is assumed to be a vector summation of errors caused by different sources, so the scalar summation of all errors together represents a worst case scenario. To estimate this calculation error, an SC layer is assumed to be 0.02 mm, and the viable dermis and dermis together are 2 mm thick, and then, the dielectric constant and the dielectric loss factor calculation error are ∼7% and ∼2%, respectively, based on Fig. 7. The thickness measurement standard deviation (±0.003 mm) of the printing paper is used for thickness error which is ±3.3%, the corresponding dielectric constant and the dielectric loss factor calculation error are ∼4% and ∼1%, respectively, based on Fig. 8. Similarly, the measured standard deviation of dielectric constant for printing paper, which is ±3.1%, was used to represent its associated dielectric constant error. This results in a calculation error for skin dielectric constant and dielectric loss factor equal to ∼0.5% and ∼2%, respectively, based on the results shown in Fig. 9. Finally, when considering all of these errors, the *total* estimated calculation error for skin dielectric constant and dielectric loss factor is ∼11.5% and ∼5%, respectively.

In addition, some simulations were also performed to determine the calculation error. In the forward calculations, the layered skin model in Fig. 11 was used along with the nominal thickness and complex permittivity of the additional layer and their variations about these nominal values (i.e., for thickness 0.09±0.003 mm). However, in the calculation of the complex permittivity of the skin, a homogeneous skin model and only the nominal thickness and complex permittivity of the additional layer were assumed. In this way, resulting errors in the calculated complex permittivity of skin due to the skin structure and the additional layer thickness and complex permittivity accuracy could be determined. The average measured results of thickness and complex permittivity of paper were then used as the nominal parameter of the additional layer, and the measured standard deviation was used as the error of thickness and complex permittivity. The complex permittivity of SC was set to that of the SC layer of palm given in [8], the complex permittivity of viable epidermis and dermis was set to those given in [18], and fat complex permittivity was set as that of infiltrated fat given in [18]. The thickness of SC and the second layer of skin were set using the previously mentioned typical values of 0.02 and 2 mm, respectively.

TABLE I

RELATIVE COMPLEX PERMITTIVITY CALCULATION ERROR FOR ADDITIONAL LAYER WITH DIFFERENT PARAMETERS

Thickness of Additional Layer (mm)	Relative Dielectric Constant of Additional Layer	Maximum Relative Dielectric Constant Calculation Error	Maximum Relative Dielectric Loss Factor Calculation Error
0.093	1.87-j0.05	15.5 %	2.8 %
0.093	1.87-j0.09	16.0 %	2.8 %
0.093	1.99-j0.05	15.7 %	3.4 %
0.093	1.99-j0.09	16.2 %	3.5 %
0.087	1.87-j0.05	10.6 %	2.7 %
0.087	1.87-j0.09	11.2 %	2.9 %
0.087	1.99-j0.05	10.8 %	5.1 %
0.087	1.99-j0.09	11.3 %	5.3 %

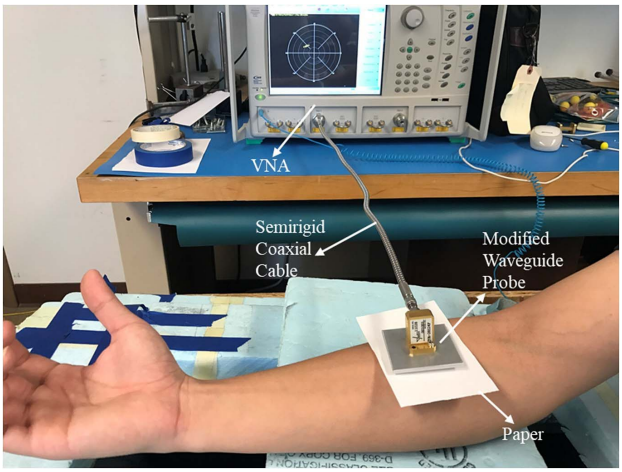

Fig. 12. Skin reflection coefficient measurement setup.

Finally, we assessed the calculation error by comparing the calculated complex permittivity results with the complex permittivity of dermis layer used in the forward calculation. The maximum calculation error for different additional layer parameters is shown in Table I. The results show that the proposed method can achieve ∼85% and ∼95% calculation accuracy for dielectric constant and dielectric loss factor, respectively, given the multiple error sources considered in these calculations.

V. *In Vivo* Human Skin Complex Permittivity Measurement Results

The measurement setup for measuring the human skin reflection coefficient is shown in Fig. 12. A piece of ordinary (70 g/m^2 white printer) paper was used to prevent skin tissue protrusion into the waveguide. The paper thickness was measured to be 0.09 ± 0.003 mm and its complex permittivity was also measured to be $(1.93 \pm 0.06) - j(0.07 \pm 0.02)$ using the method given in [12]. Slight pressure was applied to keep a good contact with the skin during the measurement. As will be seen later, we checked to ensure that applying additional pressure did not change the complex reflection coefficient measurements (over the measured frequency band). Then, the following locations were measured a *Ka*-band (26.5–40 GHz) on three human subjects, namely, forearm,

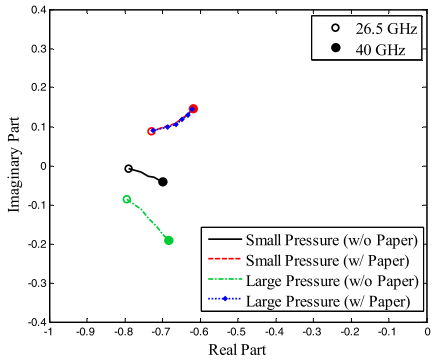

Fig. 13. Measured reflection coefficient results for different levels of pressure.

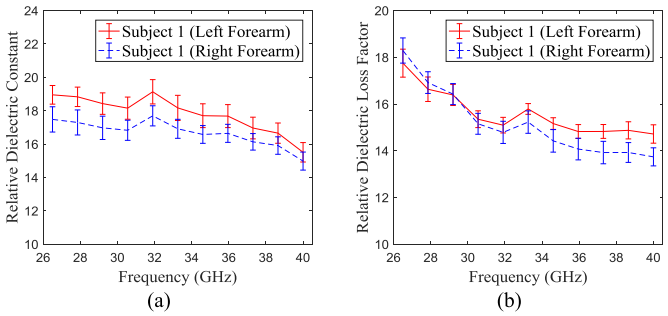

Fig. 14. Relative complex permittivity calculation results of subject 1. (a) Relative dielectric constant of the forearm. (b) Relative dielectric loss factor of the forearm.

shoulder, abdomen, thigh, calf, palm (close to thumb), and palm (close to pinky). All the experiments in this paper were performed in accordance with the guidelines of and approved by the Institutional Review Board, Missouri University of Science and Technology.

The effectiveness of using a thin layer of paper as the additional layer for eliminating the issue of pressure was examined first. The reflection coefficient of the human forearm was measured using the setup shown in Fig. 12. Two cases were examined where a small and a large amount of pressure were applied to the waveguide probe, with a thin layer of paper and with no paper. The results are shown in Fig. 13, where it can be seen that by adding just one thin layer of ordinary (printing) paper, the problem associated with pressure is completely resolved. Furthermore, the trend of the measured reflection coefficient without paper is quite similar to the simulated results shown in Fig. 5. This also validates the model used for assessing the effect of pressure (see Fig. 4).

When performing measurements on the human subjects, five measurements were taken at each location, and then, the complex permittivity was calculated for each measurement, resulting in the average and standard deviation of calculated complex permittivity for each location. The homogeneous skin model was used for all calculations. The results for the complex permittivity of the forearm of subject 1 are given in Fig. 14. The results show a very similar complex permittivity for the right and left forearms (at relatively the same locations). This is generally true for all results obtained in this paper. Therefore, for the remaining measurements, the results of the right and left forearms are all averaged together.

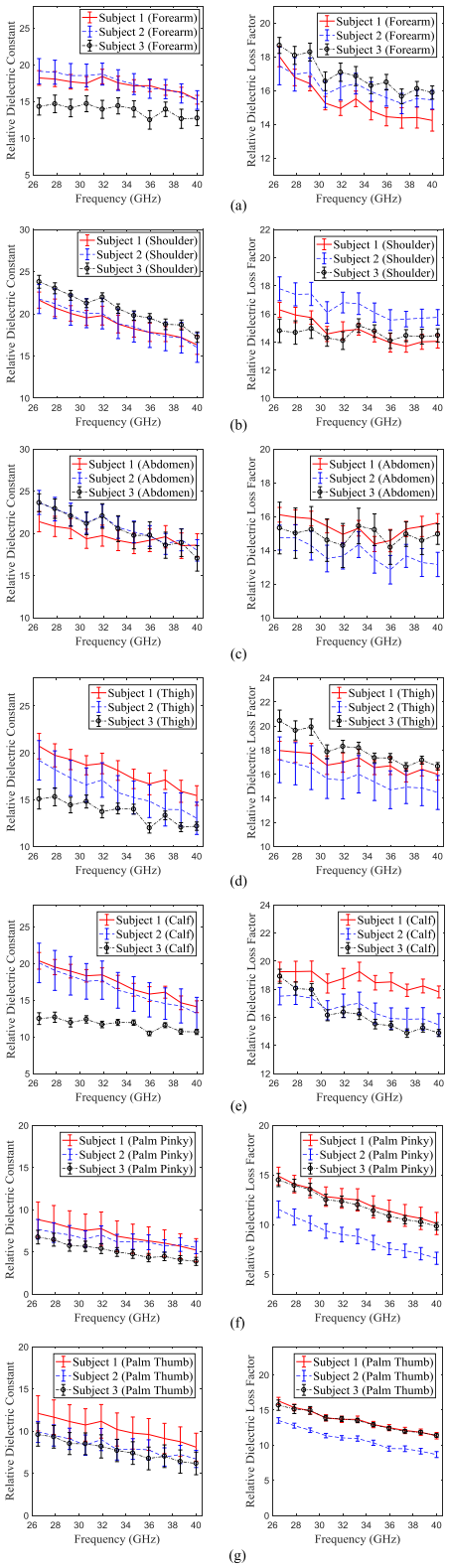

Fig. 15. Relative dielectric constant and relative dielectric loss factor calculation results for (a) forearm, (b) shoulder, (c) abdomen, (d) thigh, (e) calf, (f) palm (close to pinky), and (g) palm (close to thumb).

Fig. 15(a)–(g) shows the results of all the calculated dielectric constant and dielectric loss factor (for the three subjects and for different locations). The results show that the complex permittivity of skin varies not only as a function of different

TABLE II
MAXIMUM STANDARD DEVIATION FOR RELATIVE COMPLEX PERMITTIVITY CALCULATIONS

Locations	Maximum Standard Deviation of Relative Dielectric Constant			Maximum Standard Deviation of Relative Dielectric Loss Factor		
	Subject 1	Subject 2	Subject 3	Subject 1	Subject 2	Subject 3
Forearm	5.7 %	9.1 %	10.3 %	2.6 %	3.2 %	2.5 %
Shoulder	6.8 %	10.9 %	3.6 %	2.7 %	3.5 %	2.9 %
Abdomen	8.2 %	7.1 %	8.9 %	2.6 %	5.0 %	4.1 %
Thigh	7.4 %	13.2 %	7.0 %	3.0 %	9.1 %	1.9 %
Calf	6.4 %	16.5 %	6.4 %	2.4 %	3.5 %	1.7 %
Palm (pinky)	26.5 %	15.9 %	12.4 %	6.0 %	7.2 %	3.9 %
Palm (Thumb)	20.4 %	15.7 %	21.7 %	3.1 %	2.7 %	2.0 %

body locations in the same subject but also from subject to subject. Furthermore, the complex permittivity of the palm is in general lower than the other locations. This is directly related to the fact that palm has a relatively thick and dry SC layer. This also indicates that that using the homogeneous skin model for calculating the complex permittivity of palm may not be exactly correct. This finding is also consistent with the previous discussions. The percentage of the standard deviation relative to the corresponding average results is given in Table II. The measured standard deviation for most cases is less than or close to the estimated maximum calculation error given in Table I. However, relative dielectric constant results of palm show a large standard deviation.

VI. MEASUREMENT METHOD FOR LAYERED SKIN MODEL

As clearly demonstrated in the discussions thus far, the skin at most of the locations may be modeled as a homogeneous layer in the *Ka*-band (26.5–40 GHz) frequency range and when using an open-ended waveguide measurements method. However, simulation results have indicated a higher calculation error for locations having a relatively thick SC layer. The measurement results presented in Section IV have also indicated that the calculated palm complex permittivity is lower than those at other locations. This is the result of palm having a relatively thicker SC layer in which case a homogeneous skin layer model does not properly represent the palm region. To show the effect of using the homogeneous model for locations with a thick SC layer, a series of additional simulations was performed. The reflection coefficient of a two-layer model with a different SC layer thickness and an infinitely thick layer for the rest of the skin was first calculated. The SC layer complex permittivity was set the same as the palm SC layer given in [8], the complex permittivity of the second layer was set at the skin complex permittivity given in [18], and the complex permittivity of skin was calculated by assuming it to be homogeneous. Fig. 16 shows the results of this analysis, illustrating that the calculated complex permittivity of skin decreases with increasing thickness of the SC layer, which is consistent with the measurement results.

In addition, the measured results are also used to examine the effects of the SC layer. A 0.05-mm-thick SC layer is

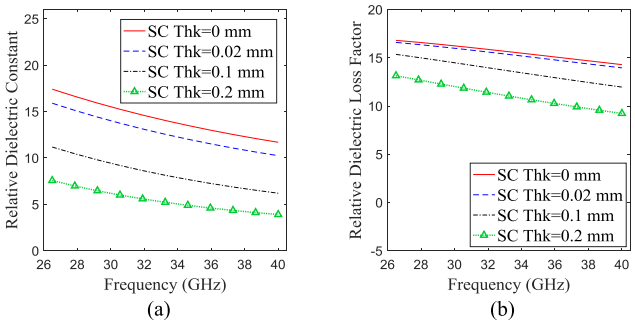

Fig. 16. Calculated relative complex permittivity by assuming a homogeneous model for layered model. (a) Relative dielectric constant. (b) Relative dielectric loss factor.

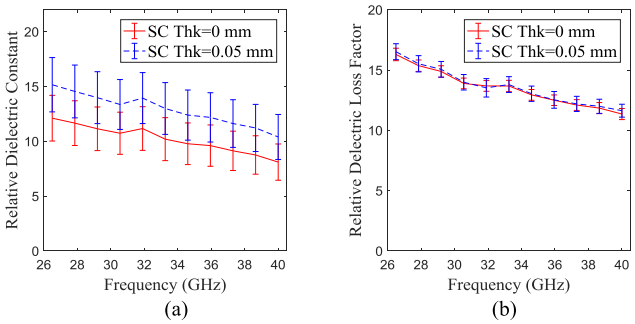

Fig. 17. Calculated relative complex permittivity by assuming homogeneous model for layered model. (a) Relative dielectric constant. (b) Relative dielectric loss factor.

assumed for palm (an area close to thumb) of subject 1, and then, the viable epidermis and dermis complex permittivity is calculated by assuming the complex permittivity of SC layer equal to the palm SC layer complex permittivity given in [8]. The calculated results are compared with the results from the homogeneous model, as shown in Fig. 17. The results indicate that by assuming an SC layer, the calculated viable epidermis and dermis complex permittivity is much higher, and it is close to the forearm complex permittivity of subject 1, as expected. Furthermore, the dielectric loss factor results do not change significantly with adding this assumed SC layer, and this phenomenon is consistent with the simulation result given in Fig. 16.

In order to correctly calculate the skin complex permittivity for the layered model, as the method in [12] is capable of doing so, one must also know the thickness of the SC layer or simultaneously solve for it as well. However, more accurate prior information can achieve a better calculation accuracy for solving the parameters in a multilayer model. For instance, if the thickness of each layer and the complex permittivity of viable epidermis and dermis are known, then the complex permittivity of SC can be calculated more accurately.

Since the SC layer on the forearm is very thin, the complex permittivity of the forearm can be seen as being equivalent to viable epidermis and dermis. Subsequently, using a secondary method, one can measure the thickness of each layer of skin (i.e., high-frequency ultrasound and Raman spectroscopy [11], [43]). Then, the only remaining unknown

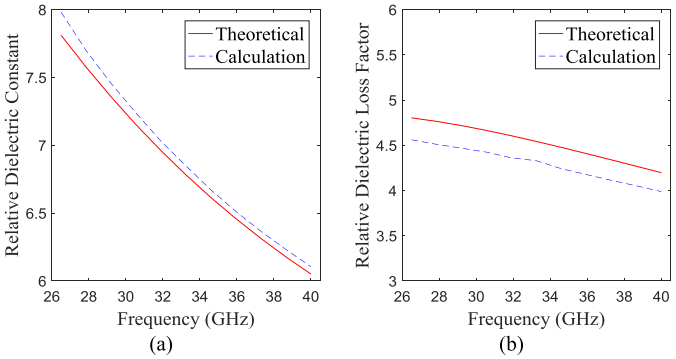

Fig. 18. Comparison of the SC layer calculated and theoretical relative complex permittivity. (a) Relative dielectric constant. (b) Relative dielectric loss factor.

parameter becomes the complex permittivity of the SC layer, which can be subsequently calculated.

To verify the proposed method, a four-layer model consisting of 0.1-mm-thick paper, 0.2-mm-thick SC layer, 2-mm-thick viable epidermis and dermis, and an infinite thick fat layer was created in CST Microwave Studio. For each layer, the complex permittivity used earlier (see Fig. 11) was considered, while the paper was assumed to be loss less with a relative dielectric constant of 2. The simulated reflection coefficient was then used to calculate the complex permittivity of SC layer knowing the thicknesses and complex permittivity of all other layers and using 43 additional higher order modes in the calculations for good convergence. The calculated results were compared with the theoretical values of SC complex permittivity used in the simulation, as shown in Fig. 18. The maximum calculation error for dielectric constant and dielectric loss factor is shown to be ∼2.2% and ∼5.3%, respectively. Considering a less number of higher order modes result in significantly higher error values, which indicates the importance of using sufficient additional higher order modes in these calculations.

VII. Conclusion

In this paper, reflectometry-based skin complex permittivity measurement methods were reviewed, indicating their strengths and shortcomings. Subsequently, comprehensive analyses were performed by considering important practical issues in an open-ended waveguide measurement approach that can significantly and adversely affect complex permittivity calculations, such as aperture field distribution approximation, finite ground plane effects, and probe pressure problem. Accordingly, a modified open-end waveguide probe method was proposed to effectively overcome these issues for skin complex permittivity measurement, in conjunction with a full-wave electromagnetic model that properly describes the interaction of the fields at the waveguide aperture with a generally layered structure (i.e., human skin). Extensive analyses were conducted to investigate and account for critical sources of error in the proposed measurement method, including assuming skin to be a homogeneous layer, thickness and complex permittivity error in an additional dielectric layer that keeps skin from protruding into the open-ended waveguide probe, and instrument noise and (operator) measurement inconsistency. The results were shown that the proposed method can achieve ∼85% and ∼95% theoretical calculation accuracy for dielectric constant and dielectric loss factor, respectively, in the *Ka*-band (26.5–40 GHz) skin complex permittivity determination. Using this robust method, skin complex permittivity on multiple body locations of three human subjects was measured. Finally, the effect of a thick SC layer in complex permittivity calculation was discussed, and a modified method to determine the complex permittivity of layered skin was proposed and verified by simulations.

References

[1] American Academy of Dermatology. (Dec. 2017). *Basic Science of the Skin*. [Online]. Available: https://www.aad.org/File%20Library/Main%20navigation/Education/Basic%20Derm%20Curriculum/revised%20files%202-2016/Basic-Science-of-the-Skin.pptx

[2] F. Töpfer, S. Dudorov, and J. Oberhammer, "Millimeter-wave near-field probe designed for high-resolution skin cancer diagnosis," *IEEE Trans. Microw. Theory Techn.*, vol. 63, no. 6, pp. 2050–2059, Jun. 2015.

[3] A. Taeb, S. Gigoyan, and S. Safavi-Naeini, "Millimetre-wave waveguide reflectometers for early detection of skin cancer," *IET Microw., Antenna Propag.*, vol. 7, no. 14, pp. 1182–1186, Nov. 2013.

[4] Y. Gao and R. Zoughi, "Millimeter wave reflectometry and imaging for noninvasive diagnosis of skin burn injuries," *IEEE Trans. Instrum. Meas.*, vol. 66, no. 1, pp. 77–84, Jan. 2017.

[5] A. Mirbeik-Sabzevari, R. Ashinoff, and N. Tavassolian, "Ultra-wideband millimeter-wave dielectric characteristics of freshly excised normal and malignant human skin tissues," *IEEE Trans. Biomed. Eng.*, vol. 65, no. 6, pp. 1320–1329, Jun. 2018.

[6] FCC. (Jul. 15. 2017). *Fact Sheet: Spectrum Frontiers Rules Identify, Open up Vast Amounts of New High-Band Spectrum for Next Generation (5G) Wireless Broadband*. [Online]. Available: https://apps.fcc.gov/edocs_public/attachmatch/DOC-340310A1.pdf

[7] F. Topfer and J. Oberhammer, "Millimeter-wave tissue diagnosis: The most promising fields for medical applications," *IEEE Microw. Mag.*, vol. 16, no. 4, pp. 97–113, May 2015.

[8] S. I. Alekseev and M. C. Ziskin, "Human skin permittivity determined by millimeter wave reflection measurements," *Bioelectromagnetics*, vol. 28, no. 5, pp. 331–339, 2007.

[9] D. B. Bennett, W. Li, Z. D. Taylor, W. S. Grundfest, and E. R. Brown, "Stratified media model for terahertz reflectometry of the skin," *IEEE Sensor J.*, vol. 11, no. 5, pp. 1253–1262, May 2011.

[10] H. Fruhstorfer, U. Abel, C. D. Garthe, and A. Knuttel, "Thickness of the stratum corneum of the volar fingertips," *Clin. Anatomy*, vol. 13, no. 6, pp. 429–433, Nov. 2000.

[11] M. Egawa, T. Hirao, and M. Takahashi, "*In vivo* estimation of stratum corneum thickness from water concentration profiles obtained with Raman spectroscopy," *Acta Dermato-Venereol.*, vol. 87, no. 1, pp. 4–8, Jan. 2007.

[12] M. T. Ghasr, D. Simms, and R. Zoughi, "Multimodal solution for a waveguide radiating into multilayered structures—Dielectric property and thickness evaluation," *IEEE Trans. Instrum. Meas.*, vol. 58, no. 5, pp. 1505–1513, May 2009.

[13] C. Gabriel, S. Gabriel, and E. Corthout, "The dielectric properties of biological tissues: I. Literature survey," *Phys. Med. Biol.*, vol. 41, no. 11, pp. 2231–2249, Nov. 1996.

[14] Keysight Technologies. (Jul. 15. 2017). *N1500A Materials Measurement Suite Technical Overview*. [Online]. Available: http://literature.cdn.keysight.com/litweb/pdf/5992-0263EN.pdf?id=2547117

[15] Keysight Technologies. (Jul. 15. 2017). *N1501A Dielectric Probe Kit 10 MHz to 50 GHz Technical Overview*. [Online]. Available: http://literature.cdn.keysight.com/litweb/pdf/5992-0264EN.pdf?id=2605692

[16] S. Gabriely, R. Lau, and C. Gabriel, "The dielectric properties of biological tissues: II. Measurements in the frequency range 10 Hz to 20 GHz," *Phys. Med. Biol.*, vol. 41, no. 11, pp. 2251–2269, 1996.

[17] C. Gabriel, "Compilation of the dielectric properties of body tissues at RF and microwave frequencies," Armstrong Lab. (AFMC) Occupational Environ. Health Directorate Radiofreq. Radiat. Division, Brooks Air Force Base, TX, USA, Tech. Rep. AL/OE-TR-1996-0004, Jul. 2017. [Online]. Available: www.dtic.mil/get-tr-doc/pdf?AD=ADA303903

[18] S. Gabriel, R. W. Lau, and C. Gabriel, "The dielectric properties of biological tissues: III. Parametric models for the dielectric spectrum of tissues," *Phys. Med. Biol.*, vol. 41, no. 11, pp. 2271–2293, 1996.
[19] C. Gabriel, T. Y. A. Chan, and E. H. Grant, "Admittance models for open ended coaxial probes and their place in dielectric spectroscopy," *Phys. Med. Biol.*, vol. 39, no. 12, pp. 2183–2200, Dec. 1994.
[20] H. Hwang, J. Yim, J.-W. Cho, C. Cheon, and Y. Kwon, "110 GHz broadband measurement of permittivity on human epidermis using 1 mm coaxial probe," in *IEEE MTT-S Int. Microw. Symp. Dig.*, Philadelphia, PA, USA, Jun. 2003, pp. 399–402.
[21] N. Chahat, M. Zhadobov, and R. R. Augustine Sauleau, "Human skin permittivity models for millimetre-wave range," *IET Electron. Lett.*, vol. 47, no. 7, pp. 427–428, Mar. 2011.
[22] T. Lahtinen, J. Nuutinen, and E. Alanen, "Dielectric properties of the skin," *Phys. Med. Biol.*, vol. 42, no. 7, pp. 1471–1472, Jul. 1997.
[23] C. Gabriel, "Comments on 'dielectric properties of the skin,"' *Phys. Med. Biol.*, vol. 42, no. 8, p. 1671, Aug. 1997.
[24] E. Alanen, T. Lahtinen, and J. Nuutinen, "Variational formulation of open-ended coaxial line in contact with layered biological medium," *IEEE Trans. Biomed. Eng.*, vol. 45, no. 10, pp. 1241–1248, Oct. 1998.
[25] E. Alanen, T. Lahtinen, and J. Nuutinen, "Measurement of dielectric properties of subcutaneous fat with open-ended coaxial sensors," *Phys. Med. Biol.*, vol. 43, no. 3, pp. 475–485, Mar. 1998.
[26] K. Sasaki, K. Wake, and S. Watanabe, "Measurement of the dielectric properties of the epidermis and dermis at frequencies from 0.5 GHz to 110 GHz," *Phys. Med. Biol.*, vol. 59, no. 16, p. 4739, 2014.
[27] K. Sasaki, M. Mizuno, K. Wake, and S. Watanabe, "Measurement of the dielectric properties of the skin at frequencies from 0.5 GHz to 1 THz using several measurement systems," in *Proc. Infr., Millim., THz Waves (IRMMW-THz)*, Hong Kong, Aug. 2015, pp. 1–2.
[28] S. Bakhtiari, S. I. Ganchev, and R. Zoughi, "Analysis of radiation from an open-ended coaxial line into stratified dielectrics," *IEEE Trans. Microw. Theory Techn.*, vol. 42, no. 7, pp. 1261–1267, Jul. 1994.
[29] S. I. Ganchev, N. Qaddoumi, S. Bakhtiari, and R. Zoughi, "Calibration and measurement of dielectric properties of finite thickness composite sheets with open-ended coaxial sensors," *IEEE Trans. Instrum. Meas.*, vol. IM-44, no. 6, pp. 1023–1029, Dec. 1995.
[30] R. Zoughi, J. R. Gallion, and M. T. Ghasr, "Accurate microwave measurement of coating thickness on carbon composite substrates," *IEEE Trans. Instrum. Meas.*, vol. 5, no. 4, pp. 951–953, Apr. 2016.
[31] M. T. Ghasr, M. J. Horst, M. Lechuga, R. Rapoza, C. J. Renoud, and R. Zoughi, "Accurate one-sided microwave thickness evaluation of lined-fiberglass composites," *IEEE Trans. Instrum. Meas.*, vol. 64, no. 10, pp. 2802–2812, Oct. 2015.
[32] G. L. Hey-Shipton, P. A. Matthews, and J. McStay, "The complex permittivity of human tissue at microwave frequencies," *Phys. Med. Biol.*, vol. 27, no. 8, pp. 1067–1071, Aug. 1982.
[33] D. K. Ghodgaonkar, O. P. Gandhi, and M. F. Iskander, "Complex permittivity of human skin *in vivo* in the frequency band 26.5–60 GHz," in *Proc. IEEE Anntenna Propag. Soc. Int. Symp.*, Salt Lake, UT, USA, Jul. 2002, pp. 1100–1103.
[34] N. Tamyis, D. K. Ghodgaonkar, and W. T. Wui, "Dielectric properties of human skin *in vivo* in the frequency range 20–38 GHz for 42 healthy volunteers," in *Proc. 28th URSI Gen. Assem.*, 2005, pp. 1–4.
[35] M. Kempin, M. T. Ghasr, J. T. Case, and R. Zoughi, "Modified waveguide flange for evaluation of stratified composites," *IEEE Trans. Instrum. Meas.*, vol. 63, no. 6, pp. 1524–1533, Jun. 2014.
[36] S. J.-P. Egot-Lemaire and M. C. Ziskin, "Dielectric properties of human skin at an acupuncture point in the 50–75 GHz frequency range: A pilot study," *Bioelectromagnetics*, vol. 32, no. 5, pp. 360–366, Jul. 2011.
[37] P. F. M. Smulders, "Analysis of human skin tissue by millimeter-wave reflectometry," *Skin Res. Technol.*, vol. 19, no. 1, pp. 209–216, Feb. 2013.
[38] N. Janssen and P. F. M. Smulders, "Design of millimeter-wave probe for diagnosis of human skin," in *Proc. 42nd Eur. Microw. Conf. (EuMC)*, Amsterdam, The Netherlands, Oct. 2012, pp. 440–443.
[39] C. Gabriel, R. H. Bentall, and E. H. Grant, "Comparison of the dielectric properties of normal and wounded human skin material," *Bioelectromagnetics*, vol. 8, no. 1, pp. 23–27, Jan. 1987.
[40] C. M. Alabaster, "Permittivity of human skin in millimetre wave band," *Electron. Lett.*, vol. 39, no. 21, pp. 1521–1522, Oct. 2003.
[41] N. Chahat, M. Zhadobov, R. Sauleau, and S. I. Alekseev, "New method for determining dielectric properties of skin and phantoms at millimeter waves based on heating kinetics," *IEEE Trans. Microw. Theory Techn.*, vol. 60, no. 3, pp. 827–832, Mar. 2012.
[42] K. J. Bois, L. F. Handjojo, A. D. Benally, K. Mubarak, and R. Zoughi, "Dielectric plug-loaded two-port transmission line measurement technique for dielectric property characterization of granular and liquid materials," *IEEE Trans. Instrum. Meas.*, vol. 48, no. 6, pp. 1141–1148, Dec. 1999.
[43] A. Laurent *et al.*, "Echographic measurement of skin thickness in adults by high frequency ultrasound to assess the appropriate microneedle length for intradermal delivery of vaccines," *Vaccine*, vol. 25, no. 34, pp. 6423–6430, Aug. 2007.

Yuan Gao (S'15) received the bachelor's degree in electrical engineering from the Hefei University of Technology, Hefei, China, in 2010, and the master's degree in electrical engineering from the Harbin Institute of Technology Shenzhen Graduate School, Shenzhen, China, in 2013. He is currently pursuing the Ph.D. degree in electrical engineering with the Missouri University of Science and Technology (Missouri S&T), Rolla, MO, USA.

He is currently a Graduate Research Assistant with the Applied Microwave Nondestructive Testing Laboratory, Missouri S&T. His current research interests include microwave- and millimeter-wave imaging, and antenna design.

Mohammad Tayeb Ghasr (S'01–M'10–SM'12) received the Ph.D. degree in electrical engineering from the Missouri University of Science and Technology (Missouri S&T), Rolla, MO, USA, in 2009.

He is currently an Assistant Research Professor with the Electrical and Computer Engineering Department, Missouri S&T. His current research interests include the area of microwave- and millimeter-wave systems and their application nondestructive testing and 3-D synthetic aperture radar imaging.

Michael Nacy (S'17) is currently pursuing the B.S.E.E. degree with the Missouri University of Science and Technology (MST), Rolla, MO, USA.

In 2017, he was an Undergraduate Research Assistant with the Applied Microwave Nondestructive Testing Laboratory, MST. His current research interests include the microwave nondestructive evaluation and development and material characterization.

Mr. Nacy is currently the IEEE Instrumentation and Measurement Society Administrative Committee Undergraduate Representative.

Reza Zoughi (S'85–M'86–SM'93–F'06) received the B.S.E.E, M.S.E.E, and Ph.D. degrees in electrical engineering (radar remote sensing, radar systems, and microwaves) from The University of Kansas, Lawrence, KS, USA.

He is currently the Schlumberger Endowed Professor of electrical and computer engineering with the Missouri University of Science and Technology (Missouri S&T), Rolla, MO, USA. He was a co-author of over 590 journal papers, conference proceedings and presentations, and technical reports. He has 18 patents to his credit.

Dr. Zoughi served as an At-Large Adcom Member and the President for the IEEE Instrumentation and Measurement Society in 2014 and 2015, respectively. He was an At-Large IEEE PSPB Member from 2016 to 2018. He is a fellow of the American Society for Nondestructive Testing (ASNT). He was a recipient of the 2007 IEEE Instrumentation and Measurement Society Distinguished Service Award, the 2009 ASNT Research Award for Sustained Excellence, and the 2011 IEEE Joseph F. Keithley Award in Instrumentation and Measurement. In 2013, he and his co-authors were the recipients of the H. A. Wheeler Prize Paper Award from the IEEE Antennas and Propagation Society. He served on the IEEE Technical Activities Board and the IEEE Publications Services and Products Board in 2015 and 2017, respectively. He served as the Editor-in-Chief for the IEEE TRANSACTIONS ON INSTRUMENTATION AND MEASUREMENT from 2007 to 2011.